SUPPLEMENTARY FIGURES

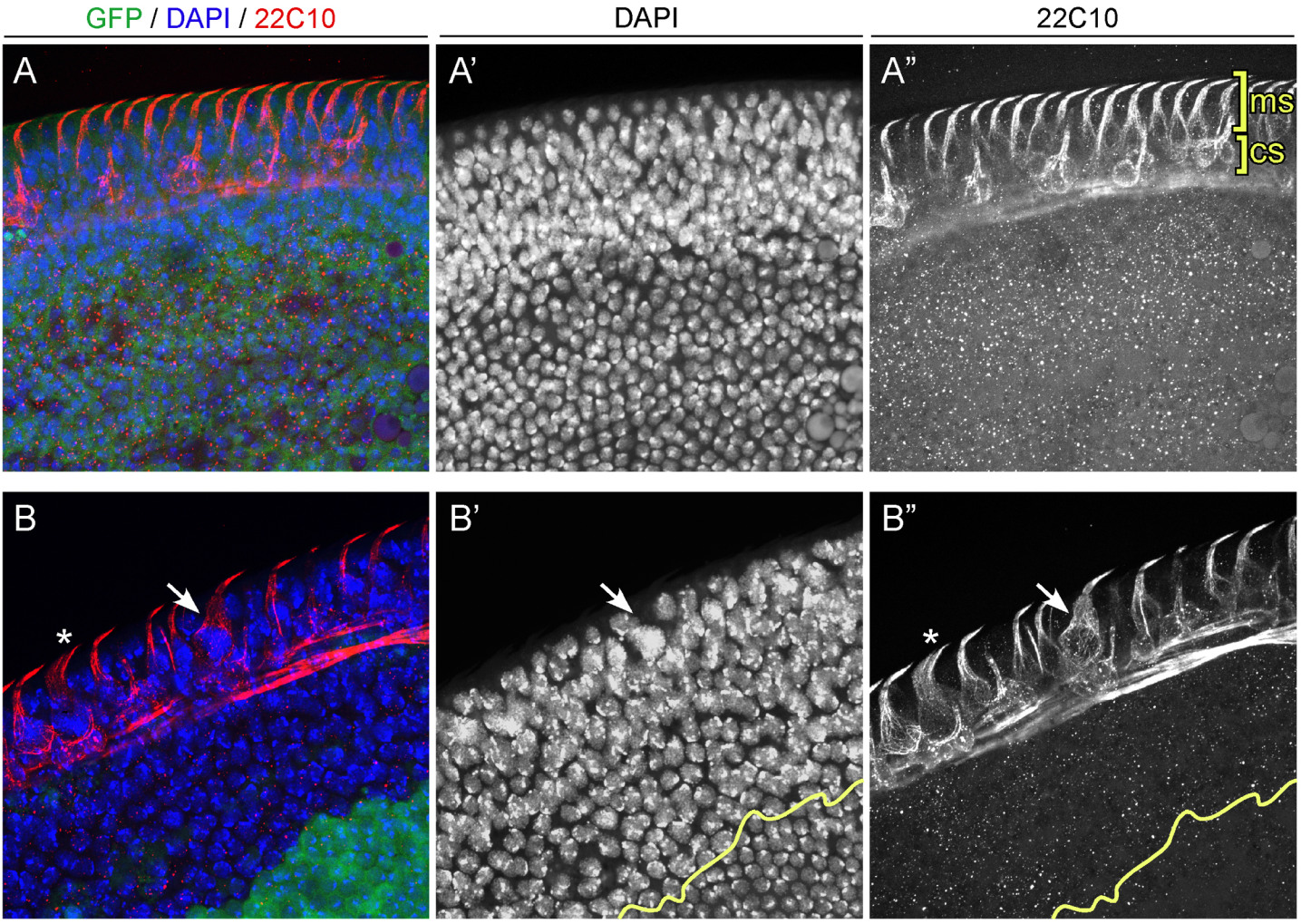

Figure S1. Abnormal nuclear and bristle morphology are displayed at the AWM of *myb* loss-of-function clones.

Shown are *myb*^{MH107} *FRT/myb*$^{+}$ *Ubi-GFP Minute FRT; hs-FLP/+* wings dissected 72 hours APF from animals reared at 18°C. **(A-A")** Control wings did not bear any clones and showed the wild-type size and distribution of nuclei (blue in A and shown in A'), as well as a wild-type pattern of sensory bristles along the AWM as visualized by 22C10 antibody (red in A and shown in A"). The mechanosensory bristles (**ms** in A") are arranged in a continuous row, with each being innervated by one neuron. Distributed below the mechanosensory bristles are the multiply innervated chemosensory bristles (**cs** in A"). **(B-B")** In *myb* clones (GFP^{-} cells in B), nuclei were larger and not as well organized (yellow line marks the clone border in B' and B"). In addition, the spacing between mechanosensory bristles in the clone was not as uniform as that in the control AWM. Asterisk indicates a double-shaft, and arrow indicates a shaft cell with an enlarged cell body.

M. K. Rovani *et al*, 2012

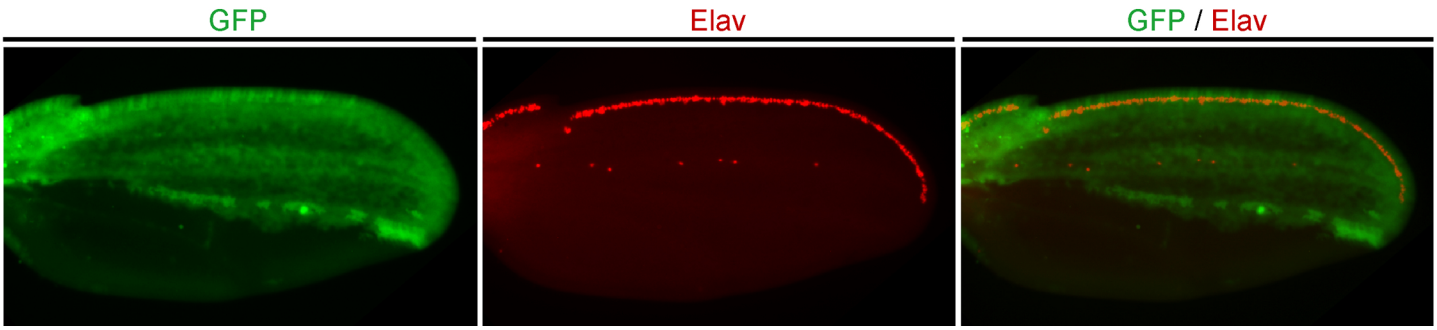

Figure S2. Ectopic-neuron phenotype at the PWM is specific to *myb* and not caused by the genetic background.

Shown is a *piMyc FRT/Ubi-GFP Minute FRT18A; hs-FLP/+* pupal wing dissected at 72 hours APF (18°C) and stained with an antibody against Elav (red) to visualize neurons. This was used as a myb^{+} genetic background control for the *FRT18A* insert since our myb^{MH107} *FRT* recombinant was generated from the *piMyc FRT18A* chromosome, and for myb^{+} clones generated in the context of a *Minute* background. As shown, *piMyc* clones, marked by lack of GFP (green), do not exhibit ectopic neurons at the PWM.

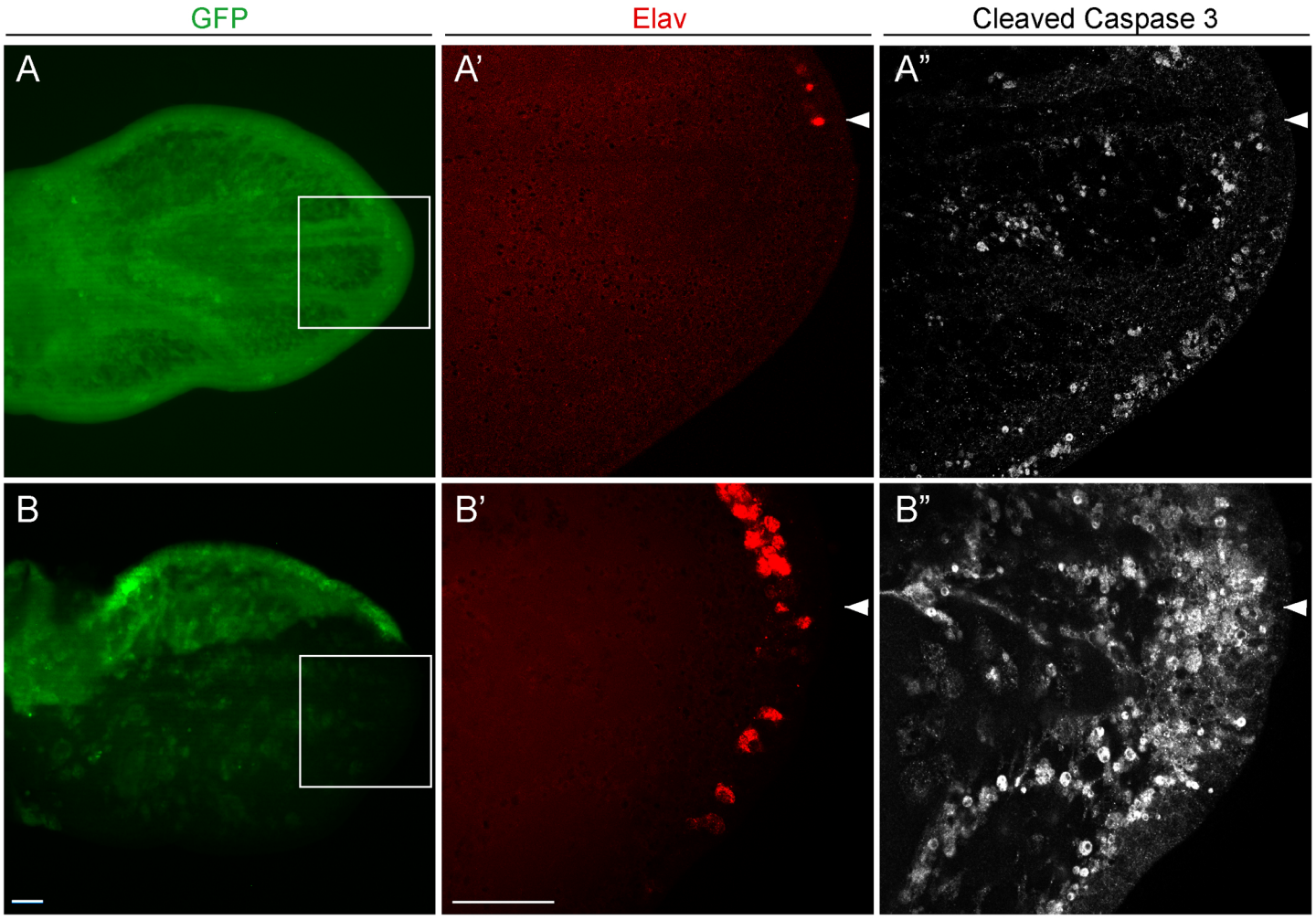

Figure S3. General apoptosis in the developing wing is not suppressed in *myb*-null clones.

Shown are pupal wings dissected at 20-24 hours APF from *myb*^{MH107} *FRT/myb*$^{+}$ *Ubi-GFP Minute FRT; hs-FLP/+* animals and stained with anti-Elav (A',B') and anti-cleaved Caspase-3 to detect cells undergoing apoptosis (A",B"). In control wings without any clones (A), neurons are not present at the PWM (A'), and apoptotic cells are present along the wing margin and more sporadically within the wing blade (A"). Pupal wing bearing a large *myb*^{MH107} clone (B) exhibited larger nuclei, ectopic neurons at the PWM (B') and higher levels of general apoptosis (B"). A'-A" and B'-B" represent the boxed areas in A and B, respectively, at a higher magnification. White arrowheads mark the distal tip of L3. Scale bars in B and B' are 0.05 mm; A, B and A'-B" are shown at the same magnifications.

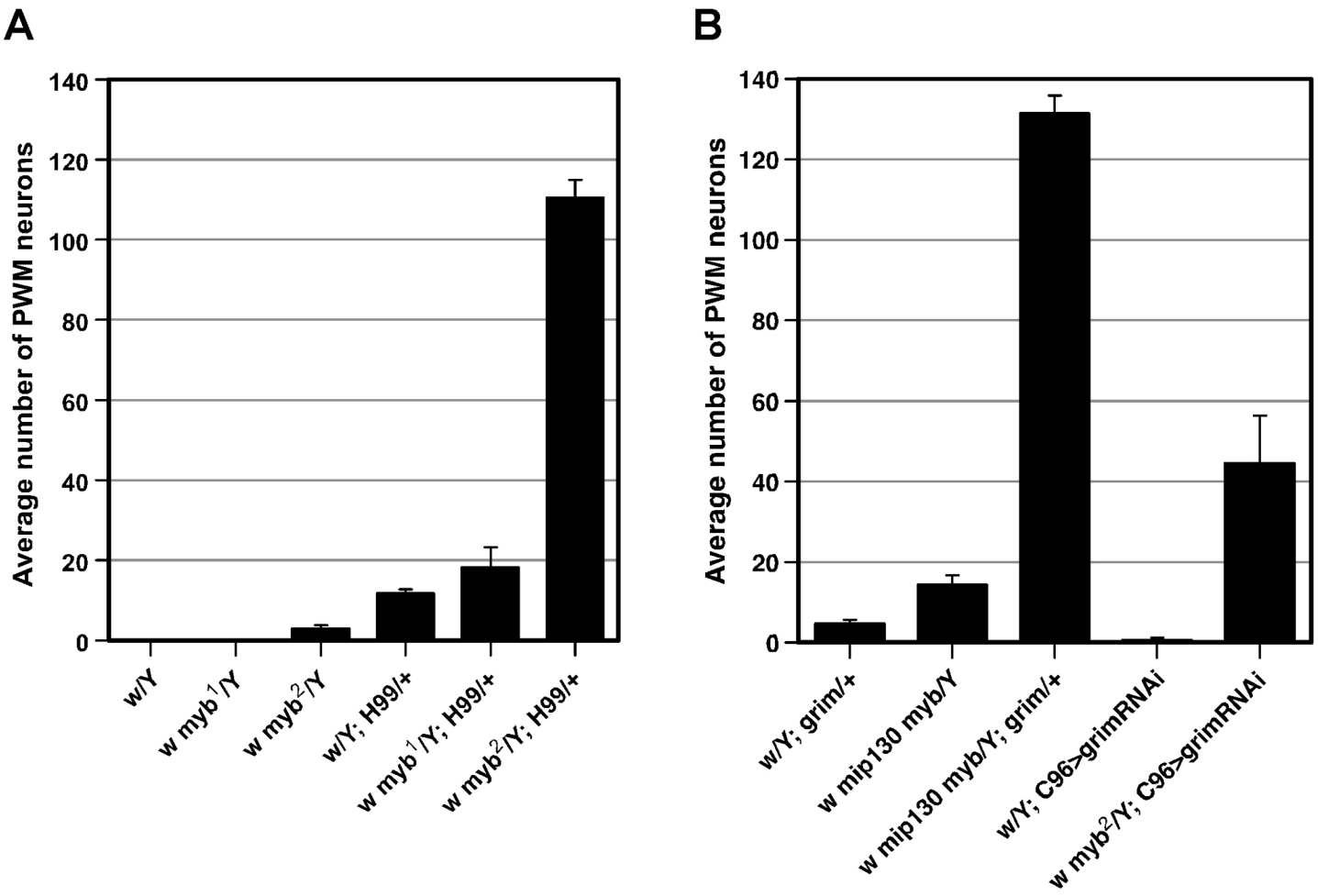

Figure S4. Genetic interaction between different mutant alleles of *Dm myb* and mutants that affect the apoptotic pathway.

(A) The *myb*^{1} allele exhibits a weaker interaction with *H99* compared to *myb*^{2}. Quantification of the number of ectopic PWM neurons in wings dissected from 72-hour APF male pupae of the indicated genotypes (18°C). **(B)** Genetic interaction between *myb* and *grim*. Quantification of the number of ectopic PWM neurons in wings dissected from 28-hour APF male pupae of the indicated genotypes, which have been abbreviated in the graph labels (24°C). Full description of the genotypes from left to right are as follows: *w/Y*; *grim*^{A6C}/+, *w mip130*$^{1-36}$ *myb*^{MH107}/Y, *w mip130*$^{1-36}$ *myb*^{MH107}/Y; *grim*^{A6C}/+, *w/Y; UAS-grimRNAi/+; C96-Gal4/+*, *w myb*^{2}/Y; *UAS-grimRNAi/+; C96-Gal4/+*. Complete loss of DMyb in *mip130*$^{1-36}$ *myb*^{MH107}; *grim*^{A6C}/+ wings led to many ectopic neurons at the PWM (ca. 132 neurons), which was an even stronger synergistic interaction than that exhibited by *myb*^{2}*; grim*^{A6C}/+ wings (ca. 83 neurons, see Fig. 7B). In addition, a similar interaction was observed using an RNAi *grim*-knockdown line.

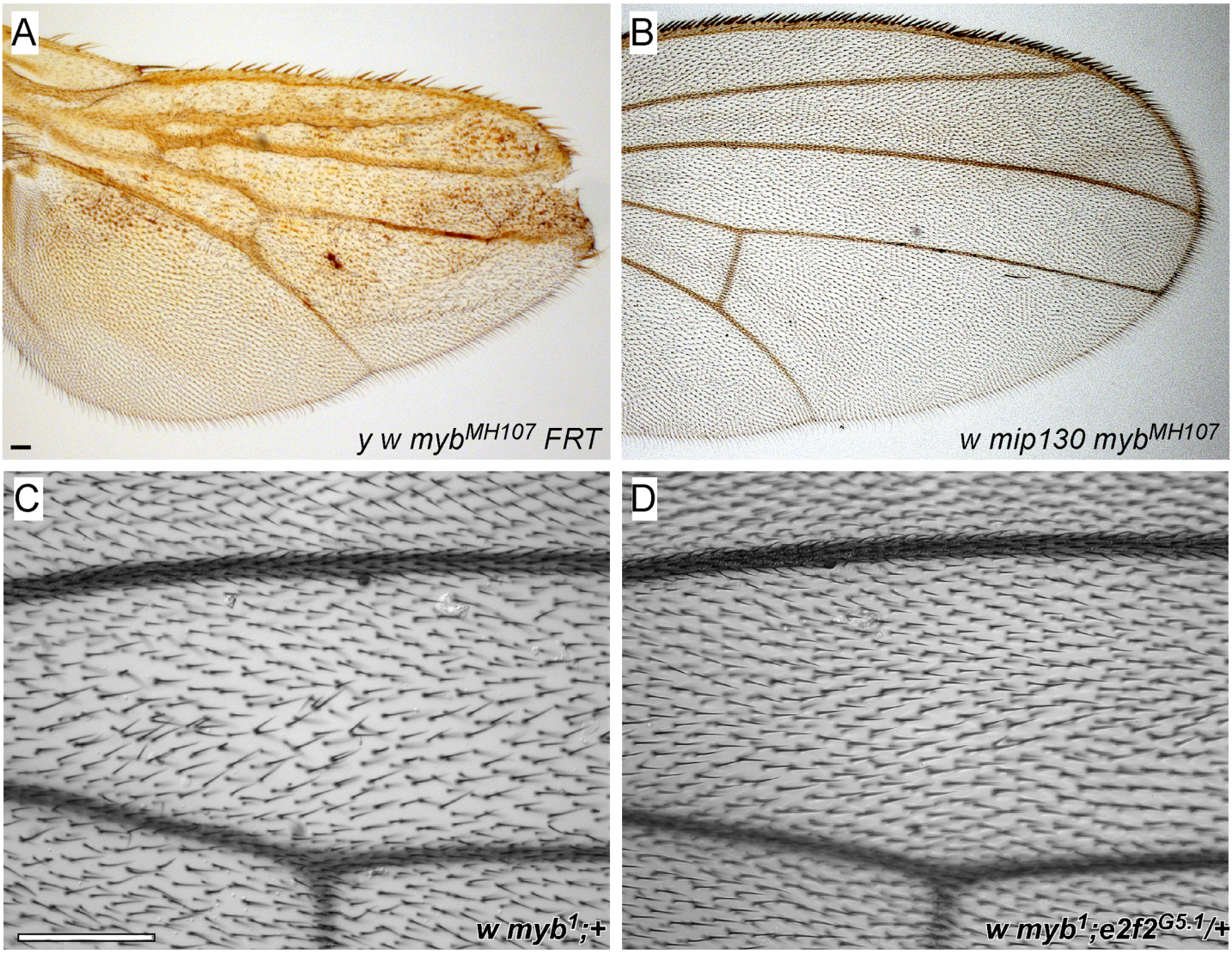

Figure S5. The cell cycle-related wing blade phenotype in *myb* mutants is suppressed by mutations in *mip130* or *de2f2*, suggesting an antagonistic relationship between these genes.

(**A-B**) Adult wings with *myb*-null clones dissected from *y* myb^{MH107} *FRT/*myb^{+} *FRT; hs-FLP/+* animals exhibited fewer wing hairs and orientation defects within the clone, phenotypes that have been shown to be associated with mitotic arrest in the mutant wing cells (A). These wing hair defects were efficiently suppressed by the absence of Mip130 in the $mip130^{1\text{-}36}$ myb^{MH107} double mutants (B). Scale bar in A is 0.05 mm, A and B are shown at the same magnification. (**C-D**) Adult wings from myb^{1} animals reared at 18°C also exhibited the cell cycle-related wing hair phenotype (C), which was suppressed by introducing a single copy of the $e2f2^{G5.1}$ mutant allele into the myb^{1} background (D). Scale bar in C is 0.1 mm; C and D are shown at the same magnification.

Figure S6. Grim levels in the developing wings are unaffected by the absence of DMyb and Mip130.

(**A-B**) Shown are eye discs (anterior left) dissected from wandering third-instar larvae and stained with antibodies against Grim (red) and Elav (green). Grim staining was observed in the posterior compartment of *GMR-grim* eye discs (A) and absent in *grim*^{A6C} discs (B), demonstrating the specificity of the antibody towards the Grim protein. Inset in each panel shows only the Grim staining of the boxed area in a higher magnification with the morphogenetic furrow indicated by a yellow arrowhead. (**C-E'**) Shown are wings dissected at 20-22 hours APF and stained with antibodies against Grim (red in C-E; grayscale in C'-E') and Elav (green in C,D; blue in E). Control *white* wings exhibited Grim staining along the wing margin and sporadically throughout the wing (C,C'), while *grim*-null wings showed lack of Grim staining (D,D'), further demonstrating the specificity of the Grim antibody. In pupal wings dissected at 20-24 hours APF from *mip130*$^{1\text{-}36}$ *myb*^{MH107} *FRT/Ubi-GFP FRT; hs-FLP/+* animals (E,E'; clone borders are delineated with dashed lines), Grim is expressed at similar levels in the wild-type and mutant cell populations, even though some ectopic neurons persist in the homozygous mutant clones (arrowheads). Scale bars in A and C are 0.5 mm; A-B and are C-E' are shown at the same magnifications.